JOURNAL OF AIRCRAFT
Vol. 33, No. 1, January–February 1996

Flow Visualization During Multiple-Axis Motions Using a Wind-Driven Manipulator

John C. Magill,* Leigh Ann Darden,† and Narayanan M. Komerath‡
Georgia Institute of Technology, Atlanta, Georgia 30332-0150

This article explores the problem of capturing vortex flow interactions that occur during coupled-axis maneuvers at finite rates. A wind-driven dynamic manipulator (WDM) has been developed to perform simultaneous motions repetitively about two degrees of freedom under open-loop or feedback control in a low-speed wind tunnel. The concept of the WDM is examined and support interference is shown to be small compared to that in conventional approaches to maneuver simulation. Vortex flow interactions occurring near the vertical fins of a 1/32-scale fighter configuration during pitch, yaw, and coupled pitch–yaw motions are explored using quantitative laser sheet videography. Large asymmetry and complex interactions are observed in the flowfield. Vortices generated by the forebody, wing leading edge, wingtip, and vertical fins are seen to interact during the coupled pitch–yaw maneuver. Maneuvers are limited to reduced frequencies below 0.036, based on wingspan. Vortex locations are seen to be accurately reproducible and to be independent of rate as expected in this regime. Even at such low rates, several transient interaction phenomena are observed, involving vortices and control surfaces. Quantification of such phenomena is demonstrated.

Introduction

IN this article we explore flow phenomena made accessible by a new device. Maneuvering concepts for future aircraft include the use of finite rate, asymmetric flow interactions to improve pointing and evasion capability. Thrust vectoring and flow control open up maneuvers that lie well outside the traditional axis-coupling rules of aircraft flight dynamics. Flow interactions during such maneuvers must be analyzed and predicted. The vortex systems over the aircraft may be expected to be highly asymmetric during a sharp sideslip or yaw maneuver combined with high angle of attack. We may expect that the vortex systems interact and move in complex fashion.

Many of these flow interactions and opportunities cannot yet be flight tested because we do not yet know how to design craft for these maneuvers. In addition to this basic logical problem, visualizing flows and precisely repeating maneuvers during flight are much more complex than performing the same tasks in ground facilities. Simulating such maneuvers in a wind tunnel poses challenges as well, which we examine here. The maneuver can be broken down into different segments based on the constraints of the support systems and measuring instruments, and the accelerations in each phase simulated separately, as a first step. There is some evidence that scaling based on the reduced-frequency concept may yield useful results. Thus, e.g., a full-scale aircraft yaw rate of 50 deg s^{-1} at a flight speed of 100 m/s translates to a scaled rate of 160 deg s^{-1} of a 1/32-scale model at a tunnel speed of 10 m/s. The problem now reduces to that of moving a model through such motions simultaneously about multiple degrees of freedom.

Presented as Paper 94-0669 at the AIAA 32nd Aerospace Sciences Meeting and Exhibit, Reno, NV, Jan. 10–13, 1994; received Feb. 26, 1995; revision received Aug. 28, 1995; accepted for publication Aug. 29, 1995.

*Ph.D. Candidate, School of Electrical Engineering, Graduate Research Assistant, School of Aerospace Engineering. Student Member AIAA.

†National Science Foundation Graduate Fellow, School of Aerospace Engineering. Student Member AIAA.

‡Professor, Aerospace Engineering. Associate Fellow AIAA.

There are several approaches to such maneuver simulation. The most obvious is to mount the model on a manipulator arm and drive it through the required motions under computer control. Mechanisms with multiple degrees of freedom must have some of the motors mounted away from the base. Wind loads during the maneuver will cause some deflection and thus the trajectory must be corrected for these errors, which increase with the maneuver rate and the square of the wind speed. Designs using stiff-armed manipulators become too heavy and bulky. Besides the obvious cost and engineering constraints, the resulting device usually becomes larger than the model, causing unacceptable levels of flow interference. A simpler approach is to use cam-driven mechanisms to simulate one aspect of one maneuver precisely and repetitively. The mechanism must then be specific to each maneuver. In contrast, a precise robotic arm would enable us to repeat, exactly, each segment of the complex maneuver as many times as desired. Thus, the transient interaction phenomena, however complex, can be converted into periodic phenomena and measured using phase-synchronized diagnostic techniques.

Previous Work

The literature base on delta wings, bodies of revolution, and complete aircraft models maneuvering at high incidence is vast. Recent work in the open literature appears to emphasize the following areas: 1) effect of pitch rate on the bursting of leading-edge vortices, 2) effects of geometric and pneumatic control techniques on vortex bursting, 3) effect of steady sideslip on vortex systems at high pitch, 4) the wing rock phenomenon, 5) derivation of stability derivatives from steady roll and rotary balance experiments, and 6) experiments on pure pitch and pure roll oscillations of wings and bodies at incidence. Systematic experiments on large-amplitude, coupled-axis maneuvers appear to be limited to the rotary-rig experiments. For this article, the support and measurement techniques employed by these researchers are of primary interest.

Orlik-Ruckemann[1] summarizes issues in the aerodynamics of agile fighter aircraft as well as methods for visualizing and measuring them. A large-amplitude, high-frequency roll oscillation apparatus, a tiltable rotary balance, and a new fast pitch apparatus are described, along with other techniques such as video analysis from flight test, and the use of radio-controlled

models dropped from helicopters. Gad-el-Hak and Ho[2] used a sting-mount with a four-bar mechanism to drive an ogive cylinder through sinusoidal pitching oscillations in a towing tank, and observed patterns of laser-induced fluorescence in dye layers in the tank. Reduced frequencies based on diameter ranged from 0.04 to 0.75. They showed the presence of at least three time scales in the unsteady flow: 1) the oscillation period, 2) the time for aftbody separation to propagate upstream, and 3) the time for crossflow effects to convect downstream. The growth–decay cycles of different vortex systems were observed and shown to affect the rate dependence of the flow. They also used the same facility to study the growth–decay cycle of the leading-edge vortex (LEV) on a delta wing[3] undergoing sinusoidal pitch oscillations in the reduced frequency range from 0.05 to 0.3.

McKernan et al.[4] studied vortex breakdown in steady flow over a 70-deg delta wing at angles of attack from 20 to 40 deg and sideslip angles up to 12 deg, quantifying breakdown positions, surface pressure distributions, and rolling moments. Asymmetric vortex breakdown was shown to contribute to the nonlinear static rolling moment characteristics, with the windward vortex breakdown moving upstream with increasing sideslip and angle of attack.

LeMay et al.[5] used a dual-rod mount and a mechanism with kinematics designed for sinusoidal pitching of a delta wing in a low-speed wind tunnel. They studied the movement of the vortex breakdown locations through the different phases of the pitch oscillation for reduced frequencies of 0.05–0.3. Soltani et al.[6] measured forces and moments on a sinusoidally oscillating 70-deg delta wing in low-speed flow, using a cam mechanism. They attributed highly nonlinear variations in the forces and rolling moments at nonzero sideslip to asymmetric vortex bursting. Static and dynamic lift measurements on thicker wing models were found to be more sensitive to Reynolds number. Reference 7 describes several rotary balance measurements of force and moment during simulated oscillations and Ref. 8 describes the measurement of pitch damping. Another application area for dynamic model manipulators is in captive-trajectory simulation of store separation and other maneuvers.[9] Here, rate effects are not generally sought, but the technique described in this article can be applied to extract force-free trajectories. In addition, rate effects may become important in future store separation problems when the launching of an all-aspect missile during a combat maneuver is considered.

Recently, interest has grown in simulating maneuvers that are not sinusoidal motions. Miller and Gile[10] described a belt-driven turntable used to perform pitch maneuvers at continuously variable rates up to 30 deg/s, with provision for ramp-type or constant angular rates of pitch. Effects of blowing along the vortex core axis on vortex bursting under dynamic pitching conditions were studied. Nonsinusoidal pitch is also important in dynamic stall.[11–16] In Ref. 16 a dc servomotor and digital servocontroller were used to move an airfoil at constant pitch-rate about the quarter chord with finite acceleration and deceleration.

Interest in coupled-axis maneuvers has also grown. Hebbar et al.[17] reported pitch rate/sideslip effects on leading-edge extension (LEX) vortices on an F/A-18 model in a water tunnel. The model support system, mounted above the tunnel, consisted of a turntable and C-strut, together providing the two degrees of freedom required. Simple pitch-ups and pitch-downs were performed at fixed yaw.

A dynamic plunge-pitch-roll model mount is described in Ref. 18. This is a stiff-armed manipulator driven by digitally controlled hydraulic actuators. Some of the complexity of developing such a device can be glimpsed from the specifications of the device: a 15,000-lb steel structure limits strut deflection to less than 0.1 in. A massive concrete foundation had to be poured specially for the device to ensure support and vibration isolation: it should be noted that the reaction of such manipulators has to be directly transmitted to the tunnel or its supports.

This summarizes the difficulty of developing a multiple-degree-of-freedom manipulator for coupled-axis maneuvers at high rates, their range of motion often restricted to circular or sinusoidal motion. Digitally controlled servo- or hydraulic systems enable arbitrary motions, but the need to achieve trajectory precision, free from deflection because of weight or aerodynamic loads, dictates the use of rigid links driven by large actuators, making the resulting device heavy, expensive, and intrusive. This last aspect can be seen from scale drawings and photographs of current facilities: dynamic flow interference is a real and bothersome phenomenon.

A series of student special problems performed under the third author's guidance in the late 1980s and early 1990s illustrated the opportunities and difficulties of coupled-axis maneuver simulation. It was found that the requirements for a manipulator to accurately simulate the high rates of future combat aircraft are beyond those offered by conventional stiff-arm manipulators. Simply put, a stiff robot capable of the needed rates of precise acceleration becomes too massive compared to the aircraft model, and causes unacceptable flow interference.

Reduced-Frequency Scaling of Maneuvers

Many vortex flow phenomena occurring on fighter configurations and delta wings at high incidence appear to obey Strouhal scaling (constant reduced frequency) over large ranges of Reynolds number and moderate ranges of subsonic Mach number. Also, much of the high-rate combat maneuvering of modern aircraft occurs at relatively low Mach numbers because of biological and structural limits on maximum acceleration. This means that low-speed wind-tunnel testing of small-scale models has considerable relevance to the development of aircraft maneuvering technology. A recent example of such Reynolds-number independence was seen in the vortex-flow fluctuation data of Ref. 19, where data obtained on 1/32, 1/7, and full-scale flight vehicles over a range of Mach number from 0.01 to 0.6 were seen to have a common Strouhal number. Thus, conversely, it should be possible to scale high-acceleration segments of full-scale maneuvers to equivalent transient motions of a small model in a low-speed tunnel. We make no claim of originality in this: the extensive research base on aeroelastic phenomena and dynamic stall has assumed the validity of such scaling for many years.

Wind-Driven Dynamic Manipulator

Our solution to the previous problem is to employ light and (inevitably) flexible manipulators and then tackle the problem of compensating dynamically for loads that would otherwise cause trajectory errors. This led to the development of the wind-driven dynamic manipulator (WDM).[20,21] A two-degree-

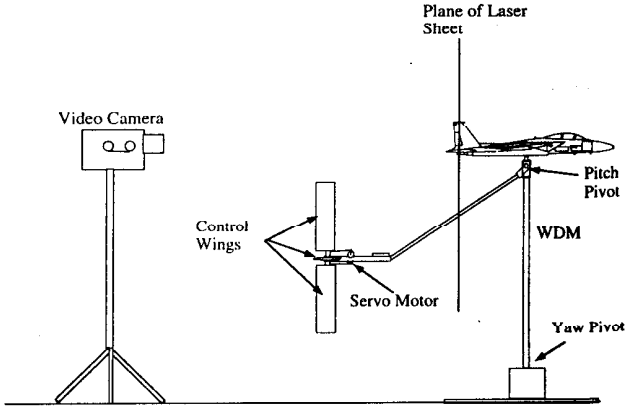

Fig. 1 Pitch–yaw manipulator and arrangement of equipment for flow visualization.

of-freedom version of the device, used for the coupled pitch–yaw maneuvers described in this article, is shown in Fig. 1. The model mount is attached to a lever arm supporting a pair of lifting control surfaces (in this case arranged orthogonally). These are pivoted at the quarter chord (to minimize required torque) and driven by small, fast model airplane servomotors. Position sensors on the model provide feedback to the control system that commands the servomotors, changing the incidence of the control surfaces. Since the control wings are light, symmetric airfoils and pivot about the quarter-chord station, very low torque is adequate to cause rapid wing motion. Also, we note that the reactions are taken by the airflow, not transmitted directly to the tunnel or its supports.

Pitch oscillations with rates up to 120 deg/s, the ability to execute step functions of pitch with minimal ringing, and the ability to command and precisely track a trajectory consisting of a sum of harmonic functions, were demonstrated in Ref. 20 at wind speeds as low as 13.3 m/s, as shown in Fig. 2. Precise trajectory tracking is simple in concept, because the maneuver can be executed several times in a wind tunnel, while one learns to shape and schedule the gains of the command function to achieve the desired result. For the flow visualization experiments of this article, the WDM was used with both open-loop radio control and closed-loop computer control to perform a series of pitch, yaw, and coupled pitch–yaw maneuvers. An i386-based microcomputer measured pitch and yaw motion from the encoder signals.

Flow Visualization

The experiments were conducted in the John J. Harper Wind Tunnel at Georgia Tech. This closed-return tunnel has a 2.1 × 2.7 m test section. The freestream speed was held at 12.5 m/s. The flow was seeded with smoke and illuminated with a laser sheet oriented perpendicular to the freestream and located just downstream of the tail of the model, where the laser sheet location is indicated by the dotted line. A video camera looked upstream at the light sheet as shown in Fig. 1. Note that the laser sheet was fixed with respect to the wind tunnel, not the model.

The personal computer display showing the instantaneous encoder readings was videotaped and mixed into a window on the flow image. Each image was thus indexed to correlate flow images with measured positions. Images were notated and enhanced for clarity using a Macintosh Quadra® computer with a frame grabber. Quantitative trajectories were extracted by manually comparing positions of given flow features with a prerecorded image of a square grid placed in the laser sheet plane. Deneba Canvas® and Adobe Photoshop® graphics software were used for this purpose.

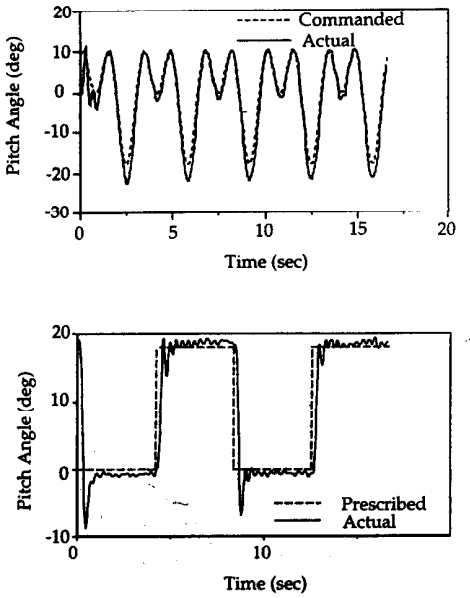

Fig. 2 Trajectory tracking with one-degree-of-freedom pitch manipulator using PID control.

Aircraft Model

The experiments were performed using a 1/32-scale YF-22 model, built from a hobby shop kit. A metal plate inside the wings is fixed to a fuselage beam and fin plates to provide rigidity. The model is filled with hardened foam and is painted flat black to minimize laser scattering, with fluorescent orange paint along the edges for visibility. The model is mounted on the WDM using a vertical rod fixed to the frame near the c.g., a support configuration chosen to minimize flow interference.

Exploration of Maneuvers

Maneuver Motion Histories

The pitch and yaw angle histories for three maneuvers are shown in Figs. 3 and 4. The displayed images are single video frames associated with instantaneous values of angles and rates. The instants of the frames are indicated by vertical arrows on the ordinate. All trajectories are presented with units of deg/s. The freestream velocity is 12.5 m/s, and the wingspan is 0.4115 m (16.2 in.). The video camera operates at 29.97 frames per second, with a shutter opening of 1 ms performed twice per frame (for the odd and even fields of horizontal lines). What is displayed here in each case is the odd or even field of a frame, thus representing a temporal resolution of 1 ms.

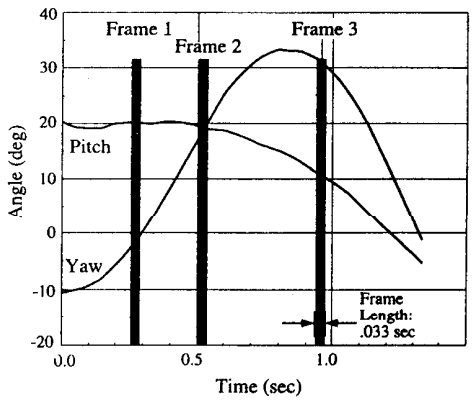

Fig. 3 Pitch and yaw histories corresponding to aircraft maneuver shown in Fig. 5.

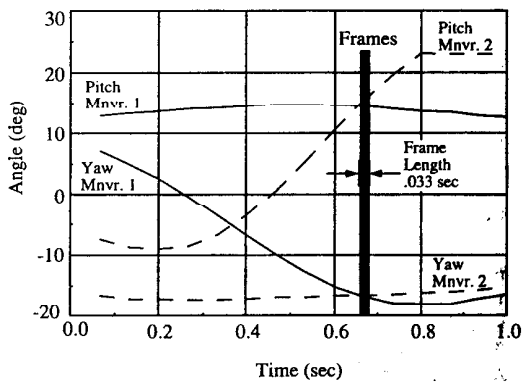

Fig. 4 Pitch and yaw histories corresponding to aircraft maneuvers shown in Fig. 7.

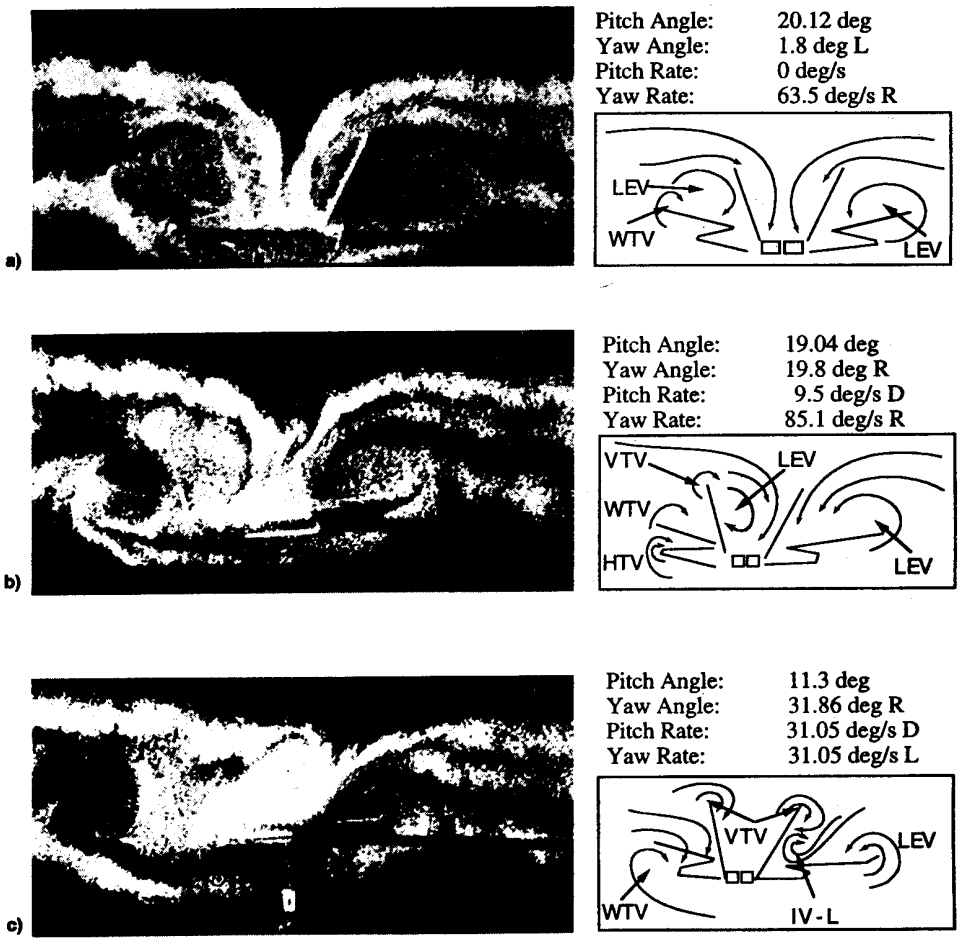

Fig. 5 Planar images of flow behind aircraft during yaw right/pitch-down maneuver. Frames a) 1, b) 2, and c) 3.

Observations

Figure 5 shows a sequence of video frames of smoke patterns in the vertical plane at the nominal wing trailing edge, as seen from downstream. The accompanying sketch is our interpretation of the observed flow features, also showing the measured instantaneous pitch and yaw angles and rates. Several types of vortices were identified in the flow images, as classified in Table 1. Type 1 is the wingtip vortex (WTV), generated at the outermost region of each wing. This is generally a small structure with a strong wake-like core that appears as a region devoid of seed particles in the laser sheet. Type 2 wing LEVs appear as two large structures at the trailing-edge visualization plane. These may or may not have a strong core, depending on the wing angle of attack, vortex burst location, and interaction effects. Type 3 is a combination leading-edge and tip vortex generated over each vertical tail (VTV) when it is yawed with respect to the local flow direction. Type 4 is a similar structure for each horizontal tail (HTV). Type 5 is a vortical structure formed above the engine inlets (IV).

The sequence in Fig. 5 captures phenomena as the aircraft undergoes a right-yaw/pitch down. In the first frame, the yaw is near zero but the flow is slightly asymmetric as a yaw rate of 63.5 deg/s has been imparted to the model. Following the first frame, the model begins a slow pitch down (9.5 deg/s) while the yaw rate increases to 85.1 deg/s. Several features appear in the second frame. The first is the huge asymmetry in the LEV system. The separatrix is inclined and the core of the LEV-L appears to be between the vertical tails. Motion of this vortex across the vertical stabilizer may be expected to produce very large time-varying loads on the tail structure. The

Table 1 Vortex phenomena-type identifiers

Type no.	Vortex type	Identifier
1	Wingtip vortex	WTV-(L or R)
2	Leading edge vortex	LEV-(L or R)
3	Vertical tail tip vortex	VTV-(L or R)
4	Horizontal tail tip vortex	HTV-(L or R)
5	Inlet vortex	IV-(L or R)

VTVs are also visible: for this severe yaw maneuver, both VTVs are to the right of the corresponding tails. In addition to the VTVs, notice the HTV-L apparently interacting with WTV-L. In the third frame of this sequence the IV-L pattern stands completely to the right of the empennage and the LEV-L can no longer be seen. The disappearance of the LEV-L results from the reduction in effective sweep of the left wing due to the large yaw angle. Further, VTV-R is clearly interacting with IV-L. The pitch-down rate in the third frame has increased to 31 deg/s. The yaw direction has been reversed.

Figure 6 plots vortex trajectories for the maneuver in Fig. 5. In each image, the vertical tail root positions were measured to locate the vortices with respect to the airframe. The sequence of the points is indicated by the arrowheads. Consecutive points are 1/15 s apart. Again LEV-L is shown to cut across both vertical stabilizers during the maneuver. The apparently sporadic movement of the WTVs is due in part to the relative motion of the wingtip with respect to the tail in a projection of the aircraft into the laser sheet plane. Interaction of two vortices (i.e., wingtip and LEVs) also causes some motion of the vortex cores.

Effects of angular rates on the flowfield can be extracted from such image data. This is demonstrated in Fig. 7, which compares two frames: one of the model at a nearly steady pitch with a moderate yaw rate of 20.5 deg/s, and a second of the model in the same position but with a small yaw rate and large pitch rate, 67.5 deg/s up. The only noticeable difference here is that the WTV-L core appears smaller and tighter in the steady-yaw image than in the high-pitch-rate image. Obviously, more quantitative measurements are needed to draw conclusions on the vortex strength and other properties, but the capability to perform qualitative comparisons is demonstrated.

Figure 8 captures the images of vortices in a plane just ahead of the vertical tails (about midchord on the wing) during a coupled pitch–yaw maneuver. A very short portion of the maneuver has been included to reveal a particular interaction phenomena. Notice in the first frame the IV-L in close proximity to the LEV-L. As the maneuver proceeds, the aircraft yaws back to the right and pitches up slightly, resulting in a rise of the LEV-L vortex core relative to that of the IV-L (frame 2). In a very short period of time (about three frames or 0.1 s) the LEV-L vortex bursts, resulting in the large gray cloud visible over the left wing in frame 3. The IV-L is still visible in the upper right corner of this cloud.

Vortex Core Trajectories and Rate Effect Analysis

By operating the WDM under feedback control a maneuver can be repeated at different rates. The motion of the vortex cores relative to the airframe can be tracked. This was done for the pair of pitch/yaw maneuvers indicated graphically in Figs. 9 and 10. The time axis for these plots has been reduced to a dimensionless parameter to compare the maneuvers. Maneuver 1 was actually completed in 4 s, while maneuver 2 took 2 s. The maximum rates achieved in maneuver 2 were ±20-deg/s pitch and ±75-deg/s yaw. A sequence of images taken during each maneuver was used to pinpoint the location of vortex cores in the plane of the laser sheet, as well as the position of the left vertical tail root projected into the same plane. Figures 11 and 12 show the location of the LEVs as the maneuvers are executed. The trajectories match quantitatively though the maneuver rates were different. This figure thus gives an integrated measure of the accuracy of the maneuver simulation using the WDM and the video-based vortex trajectory measurements.

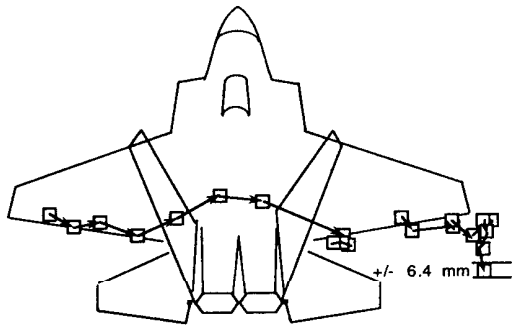

Fig. 6 Trajectory of LEVs in planar cross section behind tail during maneuver in Fig. 5. Data points are 1/15 s apart.

Error Bounds

Measurement errors in these experiments were one of three types: 1) trajectory measurement error, 2) vortex core position error, and 3) video frame/data sample misalignment. The uncertainty in measuring the pitch and yaw angles was 0.1 deg. This is dominated by noise in the signal from the position sensor. The largest error in the vortex trajectory tracking is in locating the core position in the video images, which capture a 650 × 500 mm area. Positions could be measured within 6.4 mm using the image analysis software. The difficulty is in identifying the vortex core during certain parts of a maneuver. This is especially difficult in frames where strong vortex interactions are occurring and vortex patterns are no longer circular. Correlation of the video frames to sampled data, accomplished using the time codes on the video images, could be accomplished within one frame period, or 1/30 s. With these error bounds, the symbol size used in the figures essentially gives the uncertainty in the presented data.

Flow Interference Due to the WDM

Since trajectory errors are compensated by a feedback circuit and do not need to support heavy motors, the support arms of the WDM are much slimmer than those of traditional model manipulators. No bulky motors are located anywhere near the model. The primary source of flow interference is thus the velocity induced by the control wings. An upper bound for this interference is easily computed. The angle-of-attack history of the control wings is available from the servocommand data, with appropriate corrections applied for the instantaneous

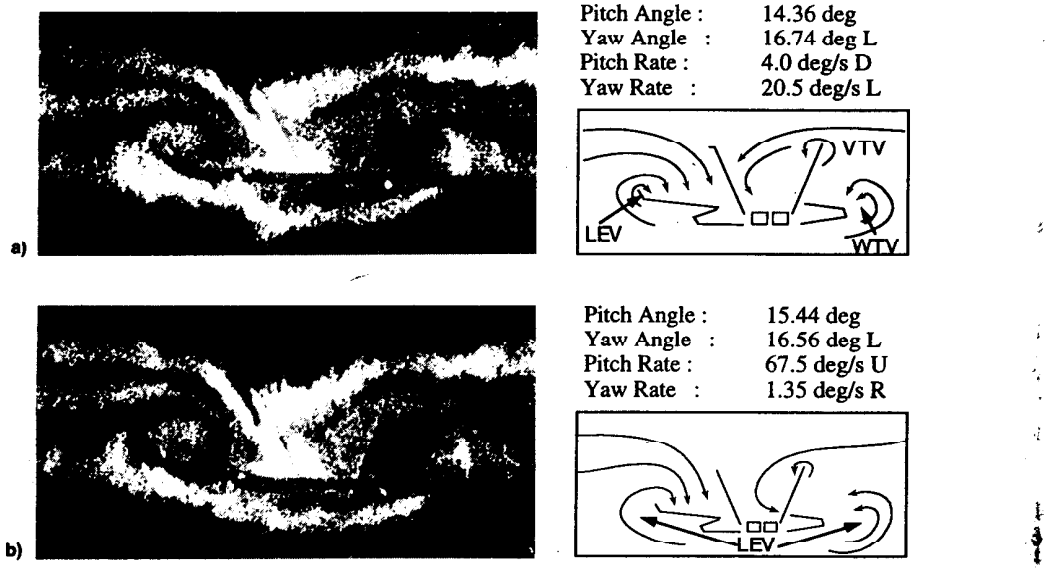

Fig. 7 Planar images of flow behind aircraft during two maneuvers. Frames a) 1 and b) 2.

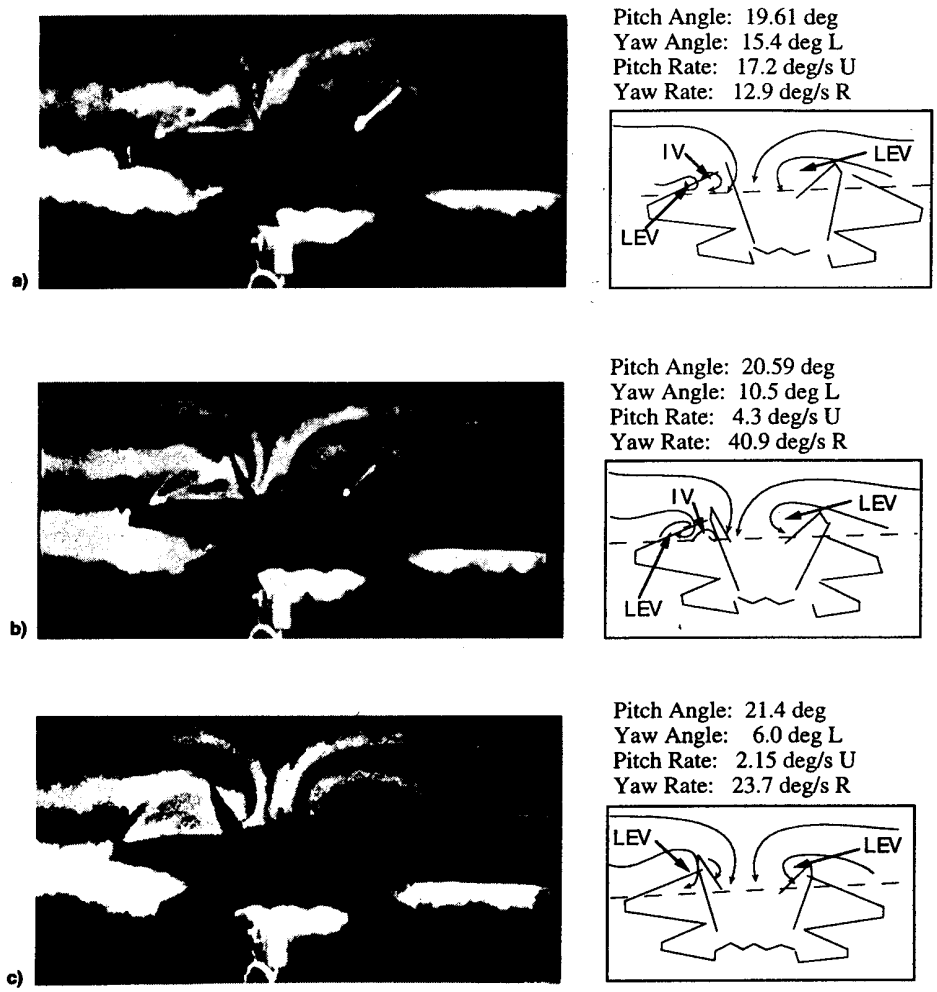

Fig. 8 Planar images of flow at midchord during left yaw–pitchdown. Frames a) 1, b) 2, and c) 3.

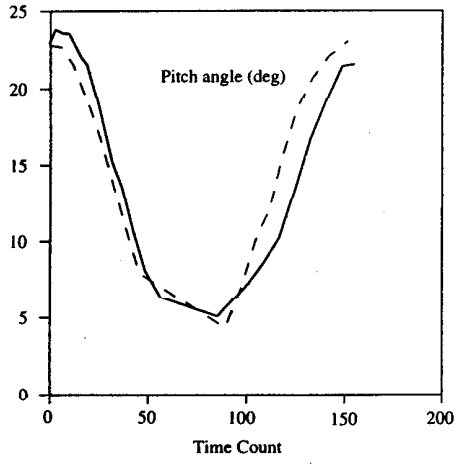

Fig. 9 Pitch angle trajectories for two maneuvers. The maneuvers were used for vortex trajectory comparisons. ——, maneuver 1 and – – –, maneuver 2. Time count, maneuver 1: 0.067 s and maneuver 2: 0.033 s.

plunge velocity. The upper bound on this angle is 10 deg. The induced velocity at the model due to the bound circulation on the wings alone is computed using a lifting-line potential flow analysis of the control wings, which are simple rectangular thin-airfoils of moderate aspect ratio. For the boom length of roughly 1 m and the tunnel speed used, the calculated induced angle of attack because of the control wings at the model location is less than 0.1 deg. This is seen to be an overestimate when the opposing effects of the trailing vortex system of the control wings are included. Obviously, the flow interference is safely negligible.

Discussion

In this article, we have been able to present some of the avenues opened by the WDM and provide a glimpse of the flow interactions occurring during aircraft maneuvers. The presentation of images and vortex trajectories in the trailing-edge plane shows only a small part of the picture, many other laser sheet orientations will be necessary to document other aspects of the interactions. Force measurements during such maneuvers are a separate issue, to be dealt with in future work: as such, no conceptual barriers are seen to performing such measurements using the WDM. Conventional strain-gauge balances can be incorporated into the boom, or more elegant schemes can be developed by modeling the system dynamics and the aerodynamics of the control wings. The vortex location measurements confirm that the maneuvers presented here are within the normally accepted limits of quasisteady analysis. The ability to quantify the vortex trajectories accurately is demonstrated using this fact. Even during such maneuvers, very rapid transient interaction phenomena are observed during these asymmetric maneuvers. Apparent vortex bursting during such interactions is also observed. These are phenomena that would probably be missed by current predictive schemes and

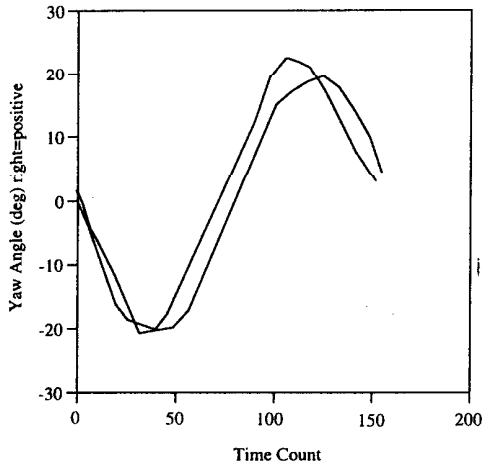

Fig. 10 Yaw angle trajectories for two maneuvers. The maneuvers were used for vortex trajectory comparisons. □, maneuver 1 and ◇, maneuver 2. Time count, maneuver 1: 0.067 s and maneuver 2: 0.033 s.

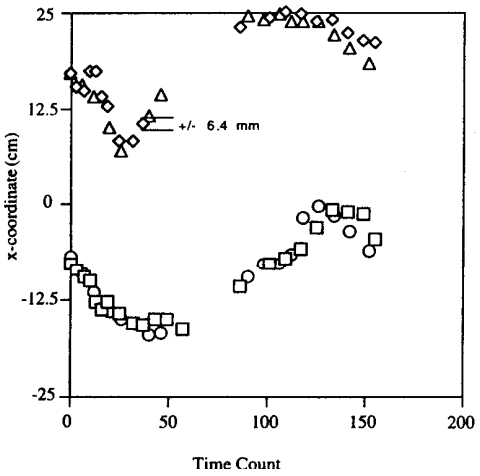

Fig. 11 Comparison of left and right LEV core positions for two maneuvers: *x* coordinate. Position is relative to left vertical tail root. □, LEV-L maneuver 1; ◇, LEV-R maneuver 1; ○, LEV-L maneuver 2; and △, LEV-R maneuver 2. Time count, maneuver 1: 0.067 s and maneuver 2: 0.033 s.

they provide a glimpse of the vast range of unknowns involved in such maneuvers.

Open-Loop vs Closed-Loop Tests

In this article, open-loop control was used to execute coupled-axis maneuvers initially, with the computer used only to track the actual trajectory using the position sensor output for analysis. For the purpose of flow visualization, this is adequate. To repeat maneuvers precisely, closed-loop control is required. To date, this has been performed using simple proportional–integral–derivative control. The testing technique is suitable for adaptive control: within a few cycles of the motion, the control system can learn to prescribe the commands needed to execute the desired trajectory precisely.

Extrapolation of WDM Capabilities for High-Rate Testing

The experiments shown here are all performed at low values of reduced frequency. This is driven by the need to perform laser sheet visualization, which works best at low flow velocity, and to validate the accuracy of the trajectory measurements using rate-independent motions. The disadvantage of the WDM is that it is wind powered: the available torque for

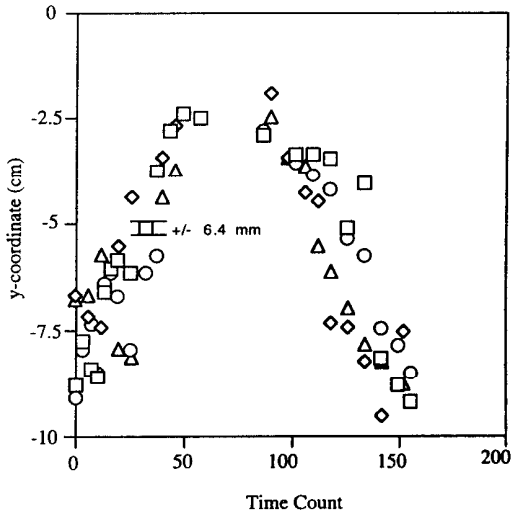

Fig. 12 Comparison of left and right LEV core positions for two maneuvers: *y* coordinate. Position is relative to left vertical tail root. □, LEV-L maneuver 1; ◇, LEV-R maneuver 1; ○, LEV-L maneuver 2; and △, LEV-R maneuver 2. Time count, maneuver 1: 0.067 s and maneuver 2: 0.033 s.

model movement depends on the dynamic pressure, which varies as the square of the tunnel speed. The maneuver rate required for a given reduced frequency varies as the first power of tunnel speed. Thus, we see that higher values of reduced frequency can be achieved by increasing tunnel speed. This is best suited for measurements of forces, moments, and dynamic stability derivatives. At low speed, higher maneuver rates can be achieved simply by using a longer moment arm and placing gears between the manipulator arm and the model mount. By the same token, the range of angle of attack achievable with a given arm length and wing size can also be increased using geared attachments.

Conclusions

1) A two-degree-of-freedom WDM has demonstrated sufficient agility to execute pitch, yaw, and coupled pitch–yaw maneuvers in a wind tunnel.

2) At reduced frequencies below 0.036 used in these experiments, no significant rate dependencies were visible in the locations of vortical flow features in the vertical plane at the wing trailing edge. This is true for several coupled pitch–yaw maneuvers studied here.

3) Vortex trajectories measured from maneuvers at different rates, within the quasisteady regime, confirm the accuracy of the WDM and video analysis techniques.

4) Even for such low maneuver rates, several transient interaction phenomena are observed in the aircraft vortex system, including sudden vortex bursting, leading to unexpected nonlinearities and nonmonotonic behavior in the quasisteady maneuver regime.

5) The WDM is seen to enable quantitative studies of the interactional aerodynamics of arbitrary maneuvers.

Acknowledgments

This work was supported under the Air Force Office of Scientific Research Grants F49620-93-1-0036 and F49620-93-1-0342. The Technical Monitors are Daniel Fant and Len Sakell. The second author acknowledges support from the National Science Foundation. The authors gratefully acknowledge the assistance provided by other members of the Experimental Aerodynamics Group at the School of Aerospace Engineering.

References

[1]Orlik-Ruckemann, K. J., "Aerodynamics of Manoeuvring Aircraft," 1992 Turnbull Lecture, *Canadian Aeronautics and Space Journal*, Vol. 38, No. 3, 1992, pp. 106–112.

[2]Gad-el-Hak, M., and Ho, C.-H., "Unsteady Flow Around an Ogive Cylinder," *Journal of Aircraft*, Vol. 23, No. 6, 1986, pp. 520–528.

[3]Gad-el-Hak, M., and Ho, C.-H., "The Pitching Delta Wing," *AIAA Journal*, Vol. 23, No. 11, 1985, pp. 1661–1665.

[4]McKernan, J. F., Payne, F. M., and Nelson, R. C., "Vortex Breakdown Measurements on a 10 Deg Sweepback Delta Wing," *Journal of Aircraft*, Vol. 25, No. 11, 1988, pp. 991, 992.

[5]LeMay, S. P., Batill, S. M., and Nelson, R. C., "Vortex Dynamics on a Pitching Delta Wing," *Journal of Aircraft*, Vol. 27, No. 2, 1990, pp. 131–138.

[6]Soltani, M. R., Bragg, M. B., and Brandon, J. M., "Measurements on a Oscillating 70-Deg Delta Wing in Subsonic Flow," *Journal of Aircraft*, Vol. 27, No. 3, 1990, pp. 211–217.

[7]Orlik-Ruckemann, K. J. (ed.), "Rotary Balance Testing for Aircraft Dynamics," AGARD Fluid Dynamic Panel Working Group 11, AGARD-AR-265, Dec. 1990.

[8]Blake, W., "Validation of the Rotary Balance Technique for Predicting Pitch Damping," AIAA Paper 93-3619, Aug. 1993.

[9]Buchanan, T. D., and Crosby, W. A., "Captive Trajectory System Test Planning for AEDC Supersonic Wind Tunnel (A) and Hypersonic Wind Tunnels (B) and (C)," Arnold Engineering and Development Center, AEDC-TR-83-40, Dec. 1983.

[10]Miller, L. S., and Gile, B. E., "Effects of Blowing on Delta Wing Vortices During Dynamic Pitching," *Journal of Aircraft*, Vol. 30, No. 3, 1993, pp. 334–339.

[11]McCroskey, W. J., "Unsteady Airfoils," *Annual Review of Fluid Mechanics*, Vol. 14, 1982, pp. 285–311.

[12]Francis, M. S., and Keesee, J. E., "Airfoil Dynamic Stall Performance with Large-Amplitude Motions," *AIAA Journal*, Vol. 23, No. 11, 1985, pp. 1653–1659.

[13]Jumper, E. J., Schreck, S. J., and Dimmick, R. L., "Lift-Curve Characteristics for an Airfoil Pitching at Constant Rate," *Journal of Aircraft*, Vol. 24, No. 10, 1987, pp. 680–687.

[14]Carr, L. W., "Progress in Analysis and Prediction of Dynamic Stall," *Journal of Aircraft*, Vol. 25, No. 1, 1988, pp. 6–17.

[15]Lorber, P. F., and Carta, F. O., "Airfoil Dynamic Stall at Constant Pitch Rate and High Reynolds Number," *Journal of Aircraft*, Vol. 25, No. 6, 1988, pp. 548–556.

[16]Koochesfahani, M. M., and Smiljanovski, V., "Initial Acceleration Effects on Flow Evolution Around Airfoils Pitching to High Angles of Attack," *AIAA Journal*, Vol. 31, No. 8, 1993, pp. 1529–1531.

[17]Hebbar, S. K., Platzer, M. F., and Cavazos, O. V., "Pitch Rate/Sideslip Effects on Leading-Edge Extension Vortices of an F/A-18 Aircraft Model," *Journal of Aircraft*, Vol. 29, No. 4, 1992, pp. 720–723.

[18]Ahn, S., Choi, K.-Y., and Simpson, R. L., "Design and Development of a Dynamic Pitch-Plunge Model Mount," AIAA Paper 89-0048, Jan. 1989.

[19]Komerath, N. M., Schwartz, R. J., and Kim, J.-M., "Flow over a Twin-Tailed Aircraft at Angle of Attack, Part II: Temporal Characteristics," *Journal of Aircraft*, Vol. 29, No. 4, 1992, pp. 553–558.

[20]Magill, J. C., and Komerath, N. M., "A Wind-Driven Dynamic Manipulator for Wind Tunnels," *Experimental Techniques*, Vol. 19, No. 1, 1995, pp. 27–30.

[21]Magill, J. C., and Komerath, N. M., U.S. Patent 5,345,818, Sept. 1994.